# Safety and efficacy of composite collagen-silver nanoparticle hydrogels as tissue engineering scaffolds

Emilio I. Alarcon, Klas I. Udekwu, Christopher W. Noel, Luke B. -P. Gagnon, Patrick K. Taylor, Branka Vulesevic, Madeline J. Simpson, Spyridon Gkotzis, Mohammed Mirazul Islam, Chyan-Jang Lee, Agneta Richter-Dahlfors, Thien-Fah Mah, Erik J. Suuronen, Juan Scaiano and May Griffith



Original Publication:

Emilio I. Alarcon, Klas I. Udekwu, Christopher W. Noel, Luke B. -P. Gagnon, Patrick K. Taylor, Branka Vulesevic, Madeline J. Simpson, Spyridon Gkotzis, Mohammed Mirazul Islam, Chyan-Jang Lee, Agneta Richter-Dahlfors, Thien-Fah Mah, Erik J. Suuronen, Juan Scaiano and May Griffith, Safety and efficacy of composite collagen-silver nanoparticle hydrogels as tissue engineering scaffolds, 2015, Nanoscale, (7), 44, 18789-18798.
http://dx.doi.org/10.1039/c5nr03826j

Nanoscale

PAPER

View Article Online
View Journal | View Issue



Cite this: *Nanoscale*, 2015, **7**, 18789

# Safety and efficacy of composite collagen–silver nanoparticle hydrogels as tissue engineering scaffolds†

Emilio I. Alarcon,*[a,b] Klas I. Udekwu,[c] Christopher W. Noel,[b] Luke B.-P. Gagnon,[d] Patrick K. Taylor,[d] Branka Vulesevic,[a] Madeline J. Simpson,[b] Spyridon Gkotzis,[c] M. Mirazul Islam,[c,e] Chyan-Jang Lee,[e] Agneta Richter-Dahlfors,[c] Thien-Fah Mah,[d] Erik J. Suuronen,[a] Juan C. Scaiano*[b,e] and May Griffith*[c,e]

Received 10th June 2015,
Accepted 29th September 2015

DOI: 10.1039/c5nr03826j

www.rsc.org/nanoscale

The increasing number of multidrug resistant bacteria has revitalized interest in seeking alternative sources for controlling bacterial infection. Silver nanoparticles (AgNPs), are amongst the most promising candidates due to their wide microbial spectrum of action. In this work, we report on the safety and efficacy of the incorporation of collagen coated AgNPs into collagen hydrogels for tissue engineering. The resulting hybrid materials at [AgNPs] < 0.4 μM retained the mechanical properties and biocompatibility for primary human skin fibroblasts and keratinocytes of collagen hydrogels; they also displayed remarkable anti-infective properties against *S. aureus*, *S. epidermidis*, *E. coli* and *P. aeruginosa* at considerably lower concentrations than silver nitrate. Further, subcutaneous implants of materials containing 0.2 μM AgNPs in mice showed a reduction in the levels of IL-6 and other inflammation markers (CCL24, sTNFR-2, and TIMP1). Finally, an analysis of silver contents in implanted mice showed that silver accumulation primarily occurred within the tissue surrounding the implant.

## Introduction

Biomaterial-associated infections are a significant healthcare problem and have been linked to medical morbidity and death.[2–6] This has motivated the development of materials with anti-infective properties, such as biomaterials loaded with antibiotics.[7] However, with the increasing number of bacteria that are resistant to antibiotics,[8] silver with historically documented anti-microbial activity has re-gained its attractiveness as an alternative to antibiotics.[9] While toxic to bacteria, it unfortunately is also toxic to mammalian cells.[9,10] More recently, therefore, silver nanoparticles (AgNPs) have been evaluated as a safer alternative to ionic silver.[1,11–20] The recent work from our team showed that in comparison with silver, biomolecule-coated, photochemically-produced AgNPs can have both bactericidal and bacteriostatic properties with almost negligible cytotoxic effects.[12] We also showed that oxidation of Ag to AgO is most likely the cause of the cytotoxic effects observed with AgNPs.[1]

Our overarching goal is to expand the safe use of AgNPs in the development of implantable hybrid-biomaterials with anti-infective properties for future use as scaffolds to enable regeneration of tissue and organs at a risk of bacterial colonization and concomitant biofilm formation like diabetic foot ulcers. Although some collagen-based materials including

[a]*Division of Cardiac Surgery, University of Ottawa Heart Institute, Ottawa, Ontario, Canada, K1Y 4W7*
[b]*Department of Chemistry and Centre for Catalysis Research and Innovation, University of Ottawa, Ottawa, Ontario, Canada, K1N 6N5.*
*E-mail: ealarcon@ottawaheart.ca, scaiano@photo.chem.uottawa.ca, may.griffith@liu.se*
[c]*Karolinska Institute, Swedish Medical Nanoscience Center, Department of Neuroscience, S-17177 Stockholm, Sweden*
[d]*Department of Biochemistry, Microbiology and Immunology, Faculty of Medicine, University of Ottawa, Ottawa, Canada*
[e]*Integrative Regenerative Medicine Centre, Department of Clinical and Experimental Medicine, Linköping University, S-58185 Linköping, Sweden*

† Electronic supplementary information (ESI) available: Representative absorption spectra of AgNP@collagen nanoparticles before and after lyophilization. Absorption spectra for the washes obtained from a 1.0 μM AgNP hydrogel over the course of 5 days. Area under the curve (AUC) calculated from the absorption spectra of 500 μm thickness collagen hydrogels prepared using different concentrations of AgNP@collagen. Selected Cryo-SEM images of BDDGE type I collagen-based hydrogels in the absence or presence of 1.0 μM AgNP. An image of a selected area of a collagen-based hydrogel prepared using $AgNO_3$ instead of AgNP@collagen nanoparticles and Live/Dead staining of human skin fibroblasts taken for 24 hours. Growth inhibition profile for *E. coli*, *S. aureus*, *S. epidermidis* and *P. aeruginosa* in the presence of hydrogels containing AgNPs. See DOI: 10.1039/c5nr03826j

Apligraf®, Dermagraft®, and Integra® are commercially available to promote regeneration, their performance in the setting of ischemia and/or infection remains questionable and difficult to interpret.[21] Thus, in the present contribution, we fabricated collagen-based hydrogels that incorporated collagen-coated AgNPs and characterized these for anti-bacterial effects *in vitro*. Further, we also examined the *in vivo* inflammatory effects and systemic silver distribution of implanted AgNP-containing hydrogels in mice to determine the safety of AgNP-containing implants for future clinical application. These materials in a near future could be used as tissue scaffolds for skin lesions such as burns and diabetic ulcers,[22,23] and the inner linings of the heart endocardium associated with implants.[24,25]

# Experimental

### Chemicals and reagents

Medical grade, porcine type I collagen (TheraCol, Sewon Cellontech, Seoul, South Korea) was lyophilized and reconstituted to make a 10 w/w% aqueous solution. The solution was then centrifuged three times at 4 °C (2500 rpm) to remove entrapped bubbles. 1,4-Butanediol diglycidyl ether (BDDGE) and silver nitrate ($AgNO_3$), were purchased from Sigma-Aldrich (Oakville, ON, Canada). Phosphate-buffered saline (PBS, pH 7.2) was prepared from tablets obtained from Calbiochem Corp., (Sigma). A 0.064 M $NaHCO_3$/0.036 $Na_2CO_3$ buffer solution was also prepared and adjusted to pH 10. Water for injection (WFI) was purchased from Millipore System and used throughout all the experiments. Collagenase was obtained from *Clostridium histolyticum* (250 U per mg solid, Sigma). 2-Hydroxy-1-[4-(2-hydroxyethoxy)phenyl]-2-methyl-1 propanone (I-2959) was a generous gift from Ciba Specialty Chemicals (Tarrytown, New York), and 4-(2-hydroxyethoxy)benzoic acid (HEBA) was synthesized according to a reported procedure,[26] as described previously.[1]

### Synthesis and characterization of collagen-stabilized silver nanoparticles

Spherical, 3.5 nm collagen coated AgNPs (AgNP@collagen) were prepared and characterized as previously described.[1] Briefly, aqueous solutions containing 0.2 mM $AgNO_3$ and I-2959 (both from 10 mM stock solutions in water) were deoxygenated through a 30 min $N_2$ purge and then 2.5 μM type I collagen was added dropwise (stock solution 10 ± 1 mg $ml^{-1}$ ≈ 33 μM) into the reaction media. The resulting solution was then purged with $N_2$ for another 20 min prior to irradiation in a LZC-4 V photoreactor (Luzchem Inc., Ottawa, Canada). Absorption spectra of the different AgNP batches were recorded immediately after AgNP synthesis (a 1.0 cm optical path length cuvette) using water as a baseline. In all cases the surface plasmon band (SPB) was around 400 ± 3.0 nm. AgNP solutions were kept at 4 °C for a maximum of five days prior to freeze-drying in a Labconco Freezone 6.0 Lyophilizer for 72 h.

### AgNP@collagen concentration estimation

Lyophilized AgNP@collagen particles (see Fig. 1) were reconstituted in a minimal volume of water and stirred overnight at 4 °C in the dark. As a control, a portion of the sample was re-diluted and the absorption spectrum was compared with the original stock AgNP solution. In all cases, the maximum of the AgNP-SPB changed by less than 2.0 nm. An approximate AgNP concentration for the original solution was calculated in a similar way to that described by us for gold nanoparticles.[27] In our calculation we have assumed total $Ag^+$ reduction to $Ag^0$ atoms and considered 3.5 ± 0.04 nm as the average diameter for AgNPs.[1] In the case of large spherical metallic clusters it can be assumed that the volume of the cluster ($V_{NP}$) is equal to $N$ times the volume of each individual atom ($V_{Atom}$):

$$V_{NP} = N \times V_{Atom} \quad \text{(i)}$$

By replacing the nanoparticle diameter and volume (see ref. 27), the number of atoms contained in a single nanoparticle can be calculated as follows:

$$N = \left(\frac{D_{NP}}{d_A}\right)^3 \quad \text{(ii)}$$

In (ii), $D_{NP}$ and $d_A$ are the nanoparticle and silver atomic diameters, respectively. In our calculations, we have used $D_{NP}$ = 3.5 and $d_A$ = 0.259 nm. This corresponds to an average of 2468 atoms per nanoparticle ($N_{Atoms}$). From this, the AgNP concentration can be calculated by applying the following formula:

$$[AgNP] = \frac{[AgNO_3]}{N_{Atoms}} \quad \text{(iii)}$$

where the $AgNO_3$ concentration was in all cases equal to $0.2 \times 10^{-3}$ mol $L^{-1}$. This calculation suggests that the nanoparticle concentration in the stock solution, prior to lyophilization, was ≈81 nM. We have used μM to report the AgNP concentration, but it can be converted to total silver concentration, by multiplying the AgNP concentration by the $N_{Atoms}$ (2468). Note that on top of the assumption of complete silver reduction, one must also account for the fact that the inner surface of a perfect sphere can be filled up to 70% with smaller spheres. Thus, the AgNP concentration could be underestimated by ≈30%. To avoid any unnecessary misinterpretation of those numbers, in this paper all silver concentrations are presented as total silver.

### Preparation of collagen hydrogels

Collagen hydrogels were prepared by using the epoxy cross-linker BDDGE under basic conditions, following a similar protocol recently described by Koh *et al.*[28] Calculated volumes of aqueous solutions of BDDGE were then added. Note that there are very few reports on the use of BDDGE as a stand-alone reagent for crosslinking collagen.[28–30] At pH 11, for example, no catalyst is needed as the reaction occurred close to the isoelectric point of the lysine residues on the collagen molecules

 

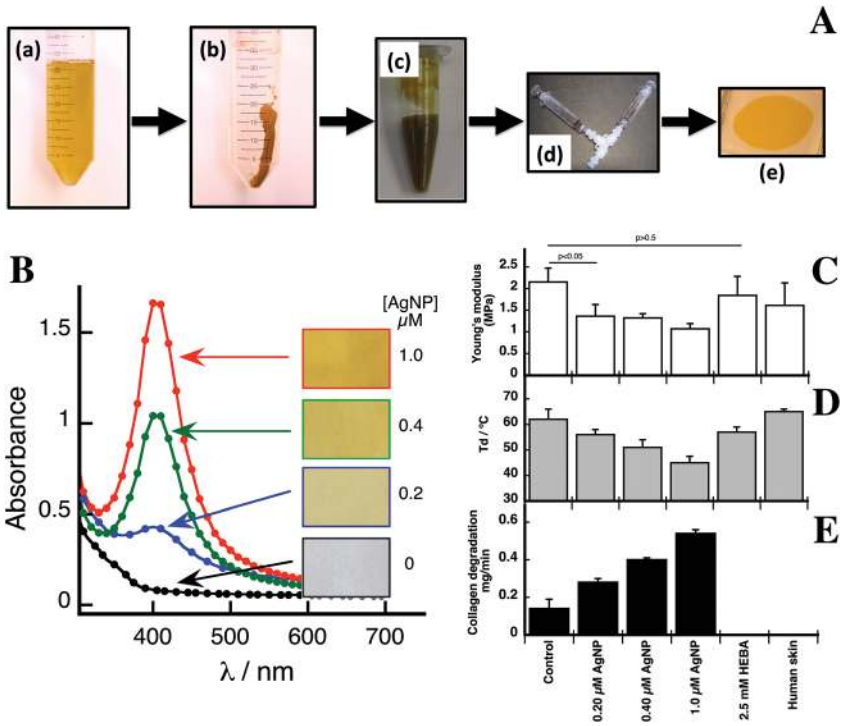


**Fig. 1** (A) Preparation of a concentrated collagen@AgNP solution and incorporation of the resulting AgNPs within a crosslinked hydrogel. (a) Tubes containing AgNP solution prepared as previously described[1] were flash-frozen and freeze-dried for three days, resulting in a yellow powder (b). This is then reconstituted in sterile water (c), mixed together with collagen using a syringe mixing system (d), crosslinked with BDDGE and then moulded into a hydrogel (e). (B) Absorption spectra of AgNP–collagen hydrogels made with different concentrations of AgNPs, measured in sterile filtered water at room temperature. The pictures correspond to an area of 10 by 5.0 mm of the actual hydrogels. In all cases the spectra were obtained after five consecutive washes of the samples. (C–E) Physical properties of BBDGE hydrogels with and without AgNP@collagen. (C) Young's modulus in MPa ($n$ = 4); (D) denaturation temperature ($T_d$, in °C) ($n$ = 4); and (E) degradation in 10 U per mL collagenase ($n$ = 4).

($pK_a$ 10–11).[31] Briefly, 0.4 ml aliquots of 10 w/w% collagen were weighed out and mixed in a T-piece system as we have previously described.[28,32,33] Collagen was buffered with 0.036 M $Na_2CO_3$ and 0.064 M $NaHCO_3$ and the pH was adjusted to 11 by titration with μl quantities of 2.0 N aqueous NaOH. Calculated volumes of aqueous solutions of BDDGE (15–25 μL) were then added to the T-piece system. The crosslinked collagen solutions were dispensed into glass moulds separated by 500 μm thick spacers (100 μm spacers were used for biofilm testing) to obtain as flat sheets, cured at 100% humidity at room temperature for 24 h, post-cured at 37 °C for 1 day, then washed extensively in PBS to remove any non-crosslinked substrate.

### Hydrogels with incorporated AgNPs or ionic silver

Collagen solutions were adjusted to pH 11 as described above. Following pH adjustment and thorough mixing, varying amounts of an 8.1 μM solution of collagen-coated AgNPs were added, see Fig. 1. As a control for specific AgNP biocompatibility and functional efficacy, hydrogels incorporating ionic silver in the form of silver nitrate ($AgNO_3$) were also prepared. The total amount of $Ag^+$ added corresponded to the total silver content found in the 0.20 μM AgNP hydrogels (494 μM). Unlike AgNPs, $AgNO_3$ is unstable under physiological conditions and will either precipitate out as silver chloride or form complexes with amine groups. Thus, two strategies were explored in the incorporation of $AgNO_3$ within the hydrogel. In the first strategy, $AgNO_3$ was directly injected into the T-piece mixing system, using a protocol similar to the one used for incorporating AgNPs. An insoluble white precipitate immediately formed which then degraded into black aggregates the following day.

In the second approach, collagen hydrogels were prepared and stored in $ddH_2O$ (not PBS). The water content within the hydrogel was exchanged for $AgNO_3$ by soaking in a $AgNO_3$ solution with a silver ion concentration that was comparable to the total silver content in the 0.20 μM AgNP hydrogel. While the material remained homogeneous and relatively clear, immediately upon the addition of either cell culture or bacterial media into the 96-well plate these hydrogels turned cloudy, suggesting that the silver precipitated as silver chloride (data not shown).

### Silver release from hydrogels

The initial silver release to the Lysogeny broth (LB) media from the hydrogels at different time intervals was determined using ICP-MS for hydrogels containing 0.2 μM AgNPs and pre-soaked with $AgNO_3$. Hydrogels without any additive were also

tested as controls. Briefly, circular pieces (6 mm in diameter) of hydrogels were placed in 10 ml of 25% LB media and incubated at 37 °C with continuous shaking. Aliquots of 1 ml were taken at the following time intervals: 0, 0.5, 1.5, 3.0 and 4.5 h. Samples were digested in a DigiPrep MS system (SCP Science) and analyzed in an inductively coupled plasma-mass spectroscopy system (ICP-MS; Agilent 7700x) and the silver content was determined by monitoring the 107 $m/z$ signal (100 ms integration). Argon was used as the carrier gas (0.85 ml $min^{-1}$, Ar plasma gas flow: 15 L $min^{-1}$). The limit of detection (LOD) of silver was determined as 0.002 μg $L^{-1}$.

### Mechanical properties and stability of composite collagen–AgNP hydrogels

The mechanical properties of the materials were evaluated by measuring the tensile strength, Young's modulus and elongation at break using an Instron Electromechanical Universal Tester (Model 3342, Instron, Norwood, MA) equipped with Series IX/S software, using a crosshead speed of 10 mm $min^{-1}$. Hydrogels were equilibrated in PBS (100 mM, pH 7.4) for 1 h before being cut into 10 × 5 mm rectangular pieces. In order to remove surface water, hydrogels were gently blotted with paper immediately prior to Instron measurements. All measurements were carried out in triplicate.

The water content of AgNP-hydrogels, previously incubated for 5 days at 4 °C, was evaluated by weighing the "wet weight" ($W_0$) of the sample. The material was then dried under vacuum at room temperature until a constant weight was achieved ($W$). The total water content of the hydrogels ($W_t$) was calculated according to the equation:

$$W_t = \frac{(W - W_0)}{W} \times 100 \quad \text{(iv)}$$

Differential scanning calorimetry measurements for hydrogels were carried out on a Q2000 Differential Scanning Calorimeter (TA Instruments, New Castle, DE) in the range of 8 to 80 °C using a scan rate of 5.0 °C $min^{-1}$. PBS-equilibrated hydrogels between 5.0 and 10 mg in mass (Sartorius CPA225D) were surface-dried with filter paper and hermetically sealed in an aluminium pan. The denaturation temperature ($T_d$) was measured at the onset of the endothermic peak. In all cases the reported data corresponded to the average of at least three independent measurements.

Material degradation by collagenase digestion was assessed by placing 50 mg of hydrated-crosslinked hydrogels in vials containing the collagenase enzyme in a PBS solution at 37 °C (5.0 ml of a 10 U per ml solution of type I collagenase). Hydrogel weights were measured at different time intervals, after the removal of surface water through blotting. The data reported in Fig. 1 correspond to the initial degradation rate of the material. Further material characterization was carried out using low temperature scanning electron microscopy (Cryo-SEM) in a Tescan (model: Vega II – XMU) with cold stage sample holder at −50 °C using a backscattered electron detector (BSE) and a secondary electron detector (SED).

### Biocompatibility and cytotoxicity assays

The *in vitro* biocompatibility and cytotoxicity of the composite hydrogels were evaluated using primary human epidermal keratinocytes (PCS-200-011, ATCC, USA) and dermal fibroblasts (PCS-201-012, ATCC, USA). Hydrogels without AgNPs served as controls. Fibroblasts were grown in Dulbecco's Modified Eagle's Medium (DMEM, Gibco) containing 10% fetal calf serum. Epidermal keratinocytes were maintained in keratinocyte serum free medium (KSFM, Gibco) for 24 h prior to the biocompatibility experiments, when the medium was changed to progenitor cell targeted epidermal keratinocyte medium, low Bovine Pituitary Extract (CnT-57, Cell-N-Tec). In order to assess the cytotoxicity as well as the ability of AgNP composites to support skin cells, hydrogels were cut into 6.0 mm circular pieces and soaked in an appropriate cell media prior to being placed into a clear bottom 96-well plate. Each sample was seeded with a 100 μl aliquot of one of either human skin keratinocytes ($5 \times 10^4$ cells per ml) or human fibroblasts ($1 \times 10^4$ cells per ml). Cell proliferation counting was carried out by using an inverted digital JuLi microscope operating in the bright field mode at days 1, 3, 5 and 7 after initial seeding, and quantification of the number of cells was carried out by using Image-J software.[11–13]

### Antimicrobial activity

The antimicrobial properties of the AgNP–collagen hydrogels were assessed against the Gram (+) bacteria *Staphylococcus aureus* (ATTC 25923) and *Staphylococcus epidermidis* (Strain Se19), as well as a Gram (−) uropathogenic strain of *Escherichia coli* (CFT073) and *Pseudomonas aeruginosa* (PAO1). In all cases, hydrogels were prepared under sterile conditions to avoid microbial contamination during the material preparation. Growth inhibition (GID) and time-kill assays (TK) were carried out using protocols designed *de novo* but inspired by the Clinical and Laboratory Standards Institute (CLSI) recommendations for antimicrobial testing.[34] Briefly, for the GID experiments, exponential cultures of each bacterium were incubated aerobically with vigorous agitation in a microplate reader (BioTek™ Synergy MX). Tested cultures of density $10^4$–$10^5$ cfu $ml^{-1}$ were seeded into 96 well plates (Falcon™) containing circular pieces of 6 mm diameter hydrogel (500 μm thickness) and bacterial growth was monitored for 18 hours at 37 °C by optical density ($\Delta OD_{600nm}$). Each experiment was carried out in duplicate and replicated at least 3 times on different days ($n \geq 6$).

For the TK assays, cultures of all three bacterial species were cultured at 37 °C overnight in a Lysogeny Broth (LB) then diluted 1 : 1000 in fresh medium. Once they reached the early exponential phase ($OD_{600nm} < 0.2$; bacteria number $\approx 10^9$ cfu $ml^{-1}$), $10^4$–$10^5$ cfu $ml^{-1}$ of bacteria were inoculated onto hydrogel samples within a 96-well plate, supplemented with 25% LB media. The samples were incubated at 37 °C with vigorous shaking and intermittent sampling in triplicate was carried out to obtain colony counts at different time intervals. Bacterial enumeration for TK was performed by manual counting of colonies growing on LB agar plates incubated at 37 °C, 24 h

 

after plating appropriate dilutions of each sample. TK data are expressed as the mean of three replicates per time point ± standard error with a limit of detection of 100 cfu $ml^{-1}$.

### Biofilm formation

Hydrogels (24 mm in diameter and 100 μm thickness) with and without 0.2 μM AgNPs were placed into the wells of a 12-well microtiter plate. Stationary phase PAO1 cultures were diluted 1 : 100 into M63 media (final concentrations of 17 mM $KH_2PO_4$, 51 mM $K_2HPO_4$, and 15 mM $(NH_4)_2SO_4$) supplemented with 0.4% arginine and 1.0 mM $MgSO_4$ inside the wells. The plate was tilted to a 45° angle to allow the biofilms to grow at the air–liquid interface (ALI) and placed at 37 °C for 16.5 hours. Following this incubation, the supernatant culture liquid was removed and the wells were washed six times with 500 μl sterile 0.9% NaCl. Next, the hydrogels were physically removed from the wells and immersed in 15 mL Falcon tubes containing 500 μl of 0.9% NaCl. The hydrogels were then vortexed for two seconds, sonicated for five minutes in a water bath sonicator, and vortexed again for another two seconds immediately before performing a spot titer assay onto LB agar plates to determine the survival CFUs. The experiments were carried out in quintuplicate using materials from different batches.

Statistical outliers were determined by constructing a box plot. Levene's test was chosen to assess whether the variances of the two populations were equal. The presence of a normal distribution was assessed through a QQ-plot. A two-sided Welch's *t*-test was utilized to determine if the difference between the mean biofilm-forming CFUs of the two populations (hydrogel and hydrogel + AgNPs) was statistically significant.

### Subcutaneous implants

All *in vivo* studies were conducted with ethical approval from the University of Ottawa Animal Care Committee and in compliance with the National Institutes of Health Guide for the Use of Laboratory Animals. Eight weeks old female C57 mice, each weighing 20–25 g, were used to assess the local reaction to the implanted hydrogels, and potential diffusion of silver particles out from the implants and systemic translocation to other sites. Briefly, hydrogels were prepared under sterile conditions and circular pieces, 6 mm in diameter, were cut and kept in sterile PBS at 4 °C until the day of surgery. During surgery, mice were anesthetized with 3.0% isoflurane through a nose cone inhaler. The back of each mouse was shaved and washed with betadine and 70% ethanol. Paravertebral incisions were made 1.0 cm away from the vertebral column. Subcutaneous pockets were created by blunt dissection using hemostats. A circular piece of hydrogel containing 0, 0.2 or 0.4 μM of AgNPs was inserted into each pocket ($n$ = 4 per group). Each incision was then closed with a 5.0 silk suture. Sham animals underwent the surgical procedure but without the implant insertion ($n$ = 3). All animals were observed for signs of inflammation; pain was managed by depot buprenorphine administered post-surgery. Mice were euthanized after 24 or 72 h. Implants and samples of different organs were collected and flash frozen for further analyses.

### Cytokine arrays

Microchip array (RayBiotech, Inc.; AAM-CYT-G3-8) analysis for the expression of 62 inflammatory and angiogenic cytokines was performed according to the manufacturer's protocol using lysates of subcutaneous tissue surrounding the implants ($n$ = 3 per group). Equal amounts of protein lysates (determined using a Pierce BCA-Kit) were loaded on the array and the levels of cytokines were calculated as fluorescence intensity relative to the internal controls. Cytokine values of experimental groups are presented as a fold-change *vs*. the sham mice.

### Inductively coupled plasma (ICP) assay for silver accumulation in murine organs

The total silver concentration in the liver, spleen, lymph nodes, kidney, and connective tissue surrounding the implant was determined using an inductively coupled plasma-mass spectroscopy system (ICP-MS; Agilent 7700x). Briefly, the organs were harvested from freshly euthanized animals in separate groups to avoid cross contamination between subjects. They were flash-frozen, powdered and subsequently freeze-dried for 48 h. The resulting powder was digested in a DigiPREP MS System (SCP Science) following the manufacturer's instructions for injection into the MS for Ag (107 $m/z$; 100 ms integration) identification (Ar carrier gas: 0.85 ml $min^{-1}$, Ar plasma gas flow: 15 L $min^{-1}$). Due to the limited amount of the solid sample and in order to improve data reliability within the same group, organs of animals within the same experimental group were pooled. The data reported here correspond to total silver determined from interpolation in a calibration curve run the same day of the experiment. The limit of detection (LOD) was 0.0093 μg $kg^{-1}$ of homogenized tissue.

### Statistical analyses

Unless otherwise indicated, in the present work, Student's *t*-test, unpaired data with unequal variance at confidence interval of $p < 0.05$ was considered as statistically significant. Analyses were carried out using KaleidaGraph 4.5®.

## Results and discussion

### Composite collagen–AgNP hydrogels

Our overarching goal was to develop a new collagen based scaffold with anti-microbial properties for use in regeneration of chronically infected/inflamed tissues. Previously, our research team developed a technique to prepare within minutes, without altering the protein conformation or increasing the oxidation extent, collagen capped silver nanoparticles using type I collagen (collagen@AgNPs). These AgNPs have superior stability in high ionic strength media and remarkable anti-bacterial properties, while retaining their biocompatibility with human cells in comparison with citrate stabilized AgNPs or silver nitrate ($AgNO_3$).[1] However, to what extent those

properties are retained in a 3D environment remains unexplored. Since we targeted the fabrication of a translatable material, we had used crosslinking strategies that have been successfully employed by our research team in the fabrication of other implantable collagen scaffolds.[28,32,33] Thus, our first candidate was the archetypical carbodiimide EDC-NHS for protein crosslinking. However, this crosslinking approach produced non-homogeneous distribution of the nanoparticles within the actual material. We attribute this to the rapid gelation of the material, within seconds (data not shown). Thus, we decided to use another crosslinking strategy with a much longer gelation time like the epoxide BDDGE crosslinking, which has a much longer gelation time (up to 12 h). In the early stages of this research, we prepared hydrogels containing AgNPs at concentrations where we observed anti-microbial activity in suspension (10–80 nM),[1] however no measurable antimicrobial activity was detected (data not shown). Thus, we have developed a *de-novo* protocol for increasing the AgNPs within the hydrogels, as shown in Fig. 1A. Our results indicate that post-injection of a AgNP concentrated solution,[35] as described in Fig. 1A, followed by the extra mixing steps after crosslinking addition produced a material with a homogeneous yellow color (Fig. 1B). By-products from the AgNP synthesis were washed out from the preparation within the first two days as shown in Fig. S2.† Meanwhile, the surface plasmon band (SPB) maximum position of AgNPs within the hydrogel was measured as 405 ± 5 nm, similar to the stock solution of AgNPs (see ref. 1) indicating that the environment for the nanoparticles is similar in solution and within the hydrogel. Further, from plotting the area under the curve for the SPB of the hydrogels, an almost linear increment was obtained with the particle concentration in the hydrogel ($R$ = 0.97, see Fig. S3†).[36]

Next, we measured the modifications on the mechanical properties and stability of hydrogels containing AgNPs, see Fig. 1C and D. We found that Young's modulus was considerably affected by the incorporation of AgNPs ($p < 0.05$). This could be due to either: (i) a decrease in the crosslinking percentage promoted by I-2959 photodecomposition products or (ii) a modification in the matrix structure due to the presence of AgNPs within the material. Experiments carried out in the presence of HEBA (the oxidation product of I-2529) at concentrations comparable to the amount expected in a hydrogel embedded with 1.0 μM AgNPs showed no differences in mechanical properties ($p > 0.5$) and/or $T_d$, ruling out possibility (i). In line with (ii), cryo-SEM imaging of the materials containing 1.0 μM AgNPs showed modifications in the material crosslinking pattern, see Fig. S4,† where a less organized crosslinking network is seen for the material containing AgNPs. Interestingly, similar Young's modulus and $T_d$ values were measured for human skin and hydrogels containing 0.2 μM AgNPs as seen in Fig. 1C and D. However, the elongation at break was higher in the skin than in the AgNP–collagen hydrogels (91 ± 23 *vs.* 43.7 ± 5.75 for skin and 0.2 μM AgNPs, respectively). Note that the stiffness results indicate that our hybrid composites are suitable candidates for use as skin scaffolds. It should also be noted that in these experiments we used a starting concentration of 10 w/w% collagen solution, whereas in the skin, the solid content is much higher due to the presence of cells, which also contribute to the mechanical properties of the tissue. While the water content of the materials remained practically unchanged (94 ± 1.0%), in line with the changes in the mechanical properties, $T_d$ values and the collagenase degradation rate were also affected by the incorporation of AgNPs. $T_d$ values were 62 ± 4 °C for the control gel, which decreased to 45 ± 2 °C for the material containing 1.0 μM AgNPs. The collagenase degradation rate changed from 0.14 to 0.54 mg $min^{-1}$ for the control and hydrogels containing 1.0 μM AgNPs, respectively (Fig. 1E). However, for the materials containing 0.2 μM AgNPs those changes were less pronounced.

### Material biocompatibility and antimicrobial performance

*In situ* cell proliferation of skin fibroblasts on hydrogels containing 0.20 μM AgNPs was unchanged from that of control hydrogels lacking AgNPs (Fig. 2A, top). Doubling the AgNP concentration to 0.40 μM, however, led to a decrease in cell proliferation. A more pronounced effect was observed for the 1.0 μM hydrogels, where by day 3 the viable cell population was significantly lower than the number of cells observed on the other gels. For epidermal skin keratinocytes the effect of AgNPs was practically independent of the nanoparticle concentration (Fig. 2A, bottom). However, materials containing 0.2 μM AgNPs demonstrated suitable compatibility for both cell lines when compared to the hydrogel containing the same total silver concentration but using $AgNO_3$ that were extremely cytotoxic, killing both epidermal and fibroblastic cells in less than 24 h (Fig. S5†). These results are consistent with the observations in the literature,[37,38] on the toxic effects of ionic silver, something not observed when our hybrid materials, at [AgNPs] < 0.4 μM, are used as scaffolds for skin cell culture. Thus, further material testing was carried out only for 0.2 and 0.4 μM AgNP hydrogels. Materials containing $AgNO_3$ (494 μM) were used for antimicrobial testing to compare the efficacy of our hybrid hydrogels.

The growth inhibition profiles for the different bacterial strains tested were compared between the prepared hydrogels and a gel impregnated with $AgNO_3$ at the same concentration as the 0.2 μM AgNP gel. The results suggest that collagen coated AgNPs retained their antibacterial properties,[1] within the BDDGE hydrogels (Fig. S6†). The estimated optical densities ($OD_{600}$) clearly demonstrated that all four bacteria were unable to grow in the presence of the hydrogels containing as little as 0.20 μM AgNPs. In contrast, each bacterium growing in wells containing control hydrogels lacking AgNPs entered log phase growth at approximately the same time as bacteria cultured in wells containing growth medium alone (data not shown). In all instances, plating for survivors at the end of each of the GIDs (18 h) did not result in the recovery of any survivors (data not shown). As this inhibition could not distinguish between bacteriostasis and bactericide, we further performed time kill (TK) experiments on each of the bacteria (Fig. 2B). The TK experiments clearly showed a decline in

 

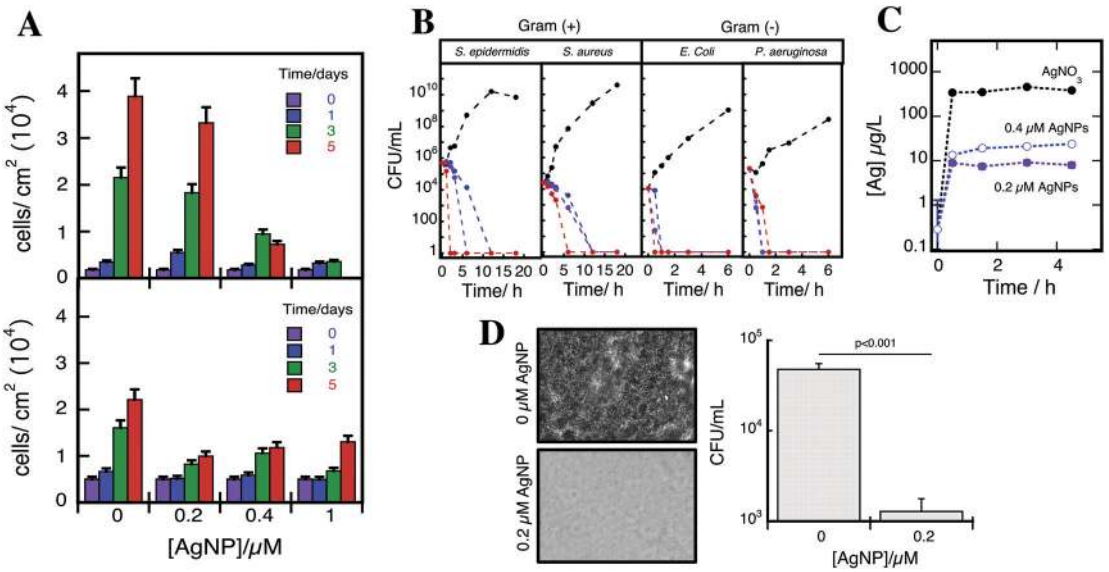


**Fig. 2** (A) Number of human skin fibroblasts (top) or keratinocytes (bottom) per cm$^2$ counted on type I collagen hydrogels at different AgNP concentrations. Error bars correspond to the standard error obtained from the average of six counts. Cells were seeded onto the surface of hydrogels containing various quantities of AgNPs. Counting was done at different time intervals after seeding for 1, 3 and 5 days. Estimated cell density immediately after seeding was included in the plot as time 0 with *a* ± 10 associated error. The cell numbers were determined from cell count data using LSM Image software. (B) Time-kill profiles for Gram (+) strains *S. epidermidis* and *S. aureus* and for Gram (–) *E. coli* and *P. aeruginosa* seeded on hydrogels for up to 18 or 6 h without (black circles), with 0.2 μM (blue circles), 0.4 μM (purple circles) and/or impregnated with $AgNO_3$ at the same total silver concentration as expected for the hydrogel at 0.2 μM AgNPs (red circles). The reported data correspond to one representative experiment with each time-point sampled in triplicate and reported as mean values ± standard error. (C) Total silver released from hydrogels containing AgNP@collagen at 0.2 and 0.4 μM incubated in 25% LB medium at 37 °C. An additional experiment using a gel impregnated with ionic silver is also included in the figure as $AgNO_3$, see the Experimental section. (D) Representative images of *P. aeruginosa* (PAO1) biofilms formed on collagen hydrogels (200 μm thickness) without and with 0.2 μM AgNPs obtained in the ALI assay at 37 °C for 16.5 hours. Right bar plot shows the colony forming units of PAO1 biofilms grown on collagen hydrogels ± AgNPs. PAO1 biofilms were grown on untreated hydrogels ($n$ = 11) and hydrogels containing 0.2 μM AgNPs ($n$ = 12). Biofilm cells were removed from the tablets *via* sonication and enumerated by a spot titer assay. Error bars correspond to the standard error. The corresponding $p$-value for a two-sided Welch's $t$-test comparing the means of the two populations is <0.001.

viable bacterial density within the first 6 h. In all cases, there was a positive correlation between the quantity of AgNPs within the hydrogel and the rate of decline in viable cell density, indicative of a concentration-dependent kill. Note that for *P. aeruginosa* the gels containing AgNPs were considerably more effective than ionic silver at eradicating the bacterial population (Fig. 2B). Further, the TK performance for the 0.2 μM AgNPs hydrogels follows the following trend *P. aeruginosa* > *E. coli* ≫ *S. epidermidis* > *S. aureus*. Overall, we have found that Gram (–) strains are far more susceptible to the antimicrobial effects of AgNPs than either *S. aureus* or *S. epidermidis* that agrees with a study by Feng *et al.*, showing *E. coli* to be more susceptible to ionic silver (*i.e.* AgNO3) than *S. aureus*.[39]

However, the question on how much silver had been effectively released from the material and how this compares within the different materials must be assessed to further evaluate the effectiveness of the hydrogels containing AgNPs. Thus, we have measured the total silver content released from the different hydrogels. Our results indicate that a steady silver concentration for all the samples is reached after ≈0.5 h of incubation, Fig. 2C. However, the total amount of silver released for the silver nitrate impregnated materials was found between 25 and 40 times higher than the amount released for the materials containing AgNP.[40] Remarkably, despite the reduced amount of released silver, the AgNP hydrogels were able to effectively control bacterial infection with comparable efficacy to that observed for ionic silver, which demonstrates the superiority of our material to circumvent silver toxicity, derived from ionic silver, in living organisms and its safety for clinical use.

Further assays for our materials involved testing of their antibiofilms using a modified air–liquid interface (ALI) assay for the *P. aeruginosa* biofilm[41] on either the control hydrogel or 0.2 μM AgNP hydrogel. Pictures taken of the hydrogels after rinsing revealed the formation of a dense biofilm layer on control hydrogels (Fig. 2D), something not observed for the materials containing AgNPs. Additional testing for the antibiofilm properties of the materials was carried out by removing the bacteria from the hydrogel surface that were later plated and enumerated, where it was observed that hydrogels containing AgNPs had significantly fewer bacteria attached to the hydrogel (≈3 log; $p$ < 0.001; Fig. 2D). This result indicates that the materials containing AgNPs are capable of hindering *P. aeruginosa* biofilm formation. Note that the ability of our materials to perform as antimicrobial and antibiofilm agents is quite rare to find, since it is usually found that much higher

concentrations of the antimicrobial agent is required to display antibiofilm properties, but in our particular case AgNPs within the material simultaneously control the bacterial population in solution and those adsorbed on the scaffold. This point presents an advantageous opportunity for future translational and biomedical applications.

### Subcutaneous implants in mouse model

Circular pieces (6 mm diameter) of hydrogels with and without 0.2 or 0.4 μM AgNPs were subcutaneously implanted dorsally in C57 mice. After 24 and 72 h the animals were sacrificed. No visual inflammation was observed for the gels containing AgNPs compared to the sham and/or control groups. Further testing for cytokine expression in the tissue surrounding the implant zone confirms these observations. Fig. 3A includes a selection of cytokines whose expression levels were statistically ($p < 0.05$) different from the sham group in the microarray after 72 h. Despite the inflammation process being an intrinsic complex mechanism, which involves cascade and signaling multi events, our data indicate that AgNPs incorporated within the collagen matrix decreased the level of expression of the pro-inflammatory cytokine IL-6 with a non-observable effect on TNFα, which reminisces the report for chronic exposure of HaCaT cells to citrate capped 50 nm AgNPs.[42] Further, added to the decrease in IL-6, we also observed a reduction in CCL24, sTNFR-2, and TIMP1, which agrees with the anti-inflammatory properties exerted by AgNPs as described by Wong *et al.*, who have shown that materials containing AgNPs are capable of reducing the inflammation in wounds, allowing faster wound healing with minimal tissue scarring.[43–45]

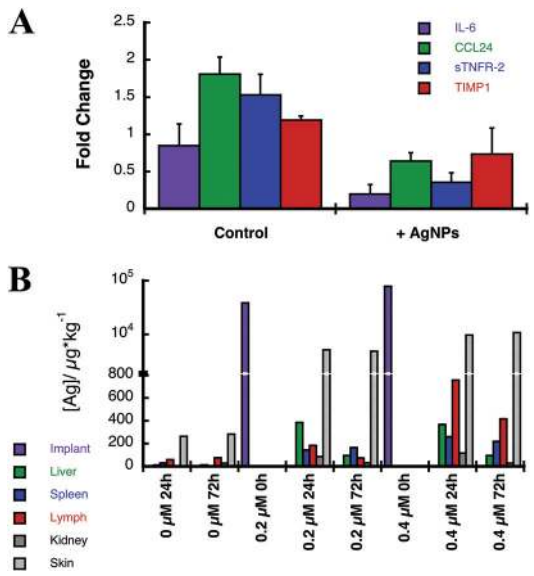


**Fig. 3** (A) Fold changes of inflammatory cytokines after 72 h implantation measured in mice homogenized skin tissues ($p < 0.05$), see the Experimental section. Error bars correspond to standard errors calculated from duplicates from three different arrays (total number of samples equal to 6). (B) Total silver content measured in selected mouse tissues/organs after 24 and 72 h subcutaneous implantation, as determined by ICP-MS. Initial silver content in the implant is included in the plot as 'Implant'. Silver concentration was estimated from direct interpolation in a calibration curve from the intensity values obtained upon injection of the digested tissue (LOD = 0.0093 μg $kg^{-1}$).

Although a direct comparison in terms of μg of silver per kg of tissue with available literature data would not be accurate due to differences in the silver source (nature of AgNPs), the total amount of silver implanted/administrated, the animal species used, and the implantation protocol/area. We also carried out experiments on silver accumulation within selected murine organs in order to explore AgNPs release from the implanted hydrogel and redistribution to other areas. The data indicate that the sub-dermal connective tissue surrounding the implant, denoted as skin in Fig. 3B, is the main reservoir for the nanoparticles. Thus, for our materials, we have found a progressive increment of silver concentration in the surrounding tissue of the implantation, reaching values of ≈12% of the initial silver content of the implant (0.2 or 0.4 μM 0 h bars in Fig. 3B). The kidney and liver, in particular have been described as central organs for the metabolism of silver in rats.[46,47] Our results indicate that at both AgNP concentrations of 0.2 and 0.4 μM, the silver concentration in the liver decreased after 72 h. Similarly, the metal concentration measured in the kidney decreased to levels close to those observed for the control group, suggesting that the silver was most likely excreted and not accumulated within that organ. Interestingly, silver accumulation in the lymph nodes for the 0.4 μM AgNPs was considerably higher than that measured for 0.2 μM. However, in both cases, the silver concentration decreases by half after 72 h reaching values close to the control group for 0.2 μM, see Fig. 3A. These observations are in line with the proposed in the literature that indicates that the toxic effects, and accumulation, of silver in living organisms are directly connected with the formation of complexes between ionic silver and key enzymes.[46] Such toxicity was expected not be observed for silver nanocrystals bound to collagen, and other extracellular matrix proteins,[46] as the case of the AgNPs herein prepared.

The preferential accumulation of silver in the surrounding area of the implant observed here reminisces of that reported by Tang *et al.*,[47] upon intracutaneous injection of AgNPs in Wistar female rats, where silver was mainly found in the subcutaneous connective tissue in the injection area. However, the silver organ profile accumulation reported by Tang *et al.*, who identified the liver and kidney, and spleen to a lesser extent, as primary reservoirs for AgNPs differs from the findings reported here. Further, the silver concentration in the spleen remained practically unchanged when compared to the other organs, which agrees with the efficient splenic capture of nanosized materials by reticular cells present in this organ.[48]

## Conclusions

We have shown that AgNPs can be stable when incorporated within a collagen hydrogel by using a slow-gelating cross-

 

linking agent. Unlike collagen hydrogels that incorporate silver ions using $AgNO_3$ as the silver source, hydrogels containing 0.2 μM AgNPs retained the biocompatibility of collagen, while displaying limited cytotoxicity. These AgNP–collagen composites possess potent bactericidal activity against *S. aureus*, *S. epidermidis*, *E. coli* and *P. aeruginosa*, and do so with a considerably smaller (25–40 × less) concentration of released silver compared to hydrogels impregnated with ionic silver. Furthermore, the materials containing 0.2 μM AgNPs were effective at preventing biofilm formation of *P. aeruginosa*. Finally, subcutaneous implants of hydrogels containing 0.2 and 0.4 μM AgNPs in mice did not produce any inflammatory response up to 72 h. Further, those materials showed a reduction in the IL-6 excretion and other inflammation markers (CCL24, sTNFR-2 and T1MP1). In terms of translocation from the implant site, silver was observed mainly in the tissue surrounding the implant. Within the first 24 h silver was also found in the liver, kidney and spleen, but the concentration in the first two organs decreased considerably after 72 h leaving yet a minimal concentration of silver within the spleen.

In summary, we have prepared a new hybrid material capable of sustaining primary skin cell proliferation with suitable physical properties to be employed as a skin scaffold that due to its remarkable anti-infective properties and non-inflammatory activity opens a new door for the treatment of tissues with a reduced regenerative ability and high risk infection rate.

## Acknowledgements

We thank our undergraduate and MSc project trainees Isabelle St-Hilaire, Rodolfo A. Elizondo, Mårten Skog, Daisy Hjelmqvist and Nadja Karamehmedovic for their excellent technical support. Funding for the project is from the Natural Sciences and Engineering Research Council of Canada through its Discovery (JCS) and CREATE (JCS, MG) programs, NSERC/CIHR Canada through its Collaborative Health Research Project program (J.C.S. and T.-F.M.), Swedish Research Council contract no. 621-2010-5189 (K.U.), Swedish Research Council (M.G.), AFA Försäkring (M.G.) and University of Ottawa Heart Institute Startup grant (E.I.A.). We would also like to express our special thanks to Michel Grenier for his assistance in taking the pictures shown in the article. J.C.S. acknowledges his appointment as visiting professor at Linköping University.

## Notes and references

1 E. I. Alarcon, K. Udekwu, M. Skog, N. L. Pacioni, K. G. Stamplecoskie, M. Gonzalez-Bejar, N. Polisetti, A. Wickham, A. Richter-Dahlfors, M. Griffith and J. C. Scaiano, *Biomaterials*, 2012, **33**, 4947–4956.
2 S. Veerachamy, T. Yarlagadda, G. Manivasagam and P. K. Yarlagadda, *Proc. Inst. Mech. Eng., Part H*, 2014, **228**, 1083–1099.
3 A. Luk, M. L. Kim, H. J. Ross, V. Rao, T. E. David and J. Butany, *Malays. J. Pathol.*, 2014, **36**, 71–81.
4 P. M. Warner, T. L. Coffee and C. J. Yowler, *Surg. Clin. North Am.*, 2014, **94**, 879–892.
5 O. Guerra, *Am. Surg.*, 2014, **80**, 489–495.
6 U. Romling, S. Kjelleberg, S. Normark, L. Nyman, B. E. Uhlin and B. Akerlund, *J. Intern. Med.*, 2014, **276**, 98–110.
7 D. Campoccia, L. Montanaro and C. R. Arciola, *Biomaterials*, 2013, **34**, 8018–8029.
8 F. C. Tenover, *Am. J. Med.*, 2006, **119**, S3–10; discussion S62–70.
9 M. Griffith, K. Udekwu, G. Spyridon, T. F. Mah and E. I. Alarcon, in *Silver Nanoparticle Applications: In the Fabrication and Design of Medical and Biosensing Devices*, ed. E. I. Alarcon, K. Udekwu and M. Griffith, Springer International Publishing, UK, 2015, ch. 5, pp. 127–146, DOI: 10.1007/978-3-319-11262-6.
10 J. W. Alexander, *Surg. Infect.*, 2009, **10**, 289–292.
11 M. J. Simpson, H. Poblete, M. Griffith, E. I. Alarcon and J. C. Scaiano, *Photochem. Photobiol.*, 2013, **89**, 1433–1441.
12 M. Vignoni, H. de Alwis Weerasekera, M. J. Simpson, J. Phopase, T.-F. Mah, M. Griffith, E. I. Alarcon and J. C. Scaiano, *Nanoscale*, 2014, **6**, 5725–5718.
13 E. I. Alarcon, C. J. Bueno-Alejo, C. W. Noel, K. G. Stamplecoskie, N. L. Pacioni, H. Poblete and J. C. Scaiano, *J. Nanopart. Res.*, 2013, **15**, 1374–1377.
14 H. Bouwmeester, J. Poortman, R. J. Peters, E. Wijma, E. Kramer, S. Makama, K. Puspitaninganindita, H. J. P. Marvin, A. A. C. M. Peijnenburg and P. J. M. Hendriksen, *ACS Nano*, 2011, **5**, 4091–4103.
15 L. C. Stoehr, E. Gonzalez, A. Stampfl, E. Casals, A. Duschl, V. Puntes and G. J. Oostingh, *Part. Fibre Toxicol.*, 2011, **8**, 3–15.
16 M. C. Moulton, L. K. Braydich-Stolle, M. N. Nadagouda, S. Kunzelman, S. M. Hussain and R. S. Varma, *Nanoscale*, 2010, **2**, 763–770.
17 W. J. Trickler, S. M. Lantz, R. C. Murdock, A. M. Schrand, B. L. Robinson, G. D. Newport, J. J. Schlager, S. J. Oldenburg, M. G. Paule and W. Slikker, *Toxicol. Sci.*, 2010, kfq244.
18 A. Travan, C. Pelillo, I. Donati, E. Marsich, M. Benincasa, T. Scarpa, S. Semeraro, G. Turco, R. Gennaro and S. Paoletti, *Biomacromolecules*, 2009, **10**, 1429–1435.
19 P. AshaRani, G. Low Kah Mun, M. P. Hande and S. Valiyaveettil, *ACS Nano*, 2008, **3**, 279–290.
20 R. Lu, D. Yang, D. Cui, Z. Wang and L. Guo, *Int. J. Nanomed.*, 2012, **7**, 2101.
21 C. Holmes, J. S. Wrobel, M. P. MacEachern and B. R. Boles, *Diabetes, Metab. Syndr. Obes.*, 2013, **6**, 17–29.
22 L. R. Mulcahy, V. M. Isabella and K. Lewis, *Microb. Ecol.*, 2014, **68**, 1–12.
23 A. Malik, Z. Mohammad and J. Ahmad, *Diabetes, Metab. Syndr. Obes.*, 2013, **7**, 101–107.
24 E. Athan, V. H. Chu, P. Tattevin, C. Selton-Suty, P. Jones, C. Naber, J. M. Miro, S. Ninot, N. Fernandez-Hidalgo,

E. Durante-Mangoni, D. Spelman, B. Hoen, T. Lejko-Zupanc, E. Cecchi, F. Thuny, M. M. Hannan, P. Pappas, M. Henry, V. G. Fowler, Jr., A. L. Crowley and A. Wang, *JAMA, J. Am. Med. Assoc.*, 2012, **307**, 1727–1735.

25 I. Van Dijck, W. Budts, B. Cools, B. Eyskens, D. E. Boshoff, R. Heying, S. Frerich, W. Y. Vanagt, E. Troost and M. Gewillig, *Heart*, 2015, **101**, 788–793.

26 X. Meng, A. Natansohn, C. Barret and P. Rochon, *Macromolecules*, 1996, **29**, 946–952.

27 N. L. Pacioni, M. Gonzalez-Bejar, E. Alarcon, K. L. McGilvray and J. C. Scaiano, *J. Am. Chem. Soc.*, 2010, **132**, 6298–6299.

28 L. B. Koh, M. M. Islam, D. Mitra, C. W. Noel, K. Merrett, S. Odorcic, P. Fagerholm, W. B. Jackson, B. Liedberg, J. Phopase and M. Griffith, *J. Funct. Biomater.*, 2013, **4**, 162–177.

29 R. Zeeman, P. J. Dijkstra, P. B. van Wachem, M. J. A. van Luyn, M. Hendriks, P. T. Cahalan and J. Feijen, *Biomaterials*, 1999, **20**, 921–931.

30 R. Zeeman, PhD, University of Twente, The Netherlands, 1998.

31 N. C. Avery, A. J. Bailey, V. H. Barocas, A. A. Biewener, R. D. Blank, A. L. Boskey, M. J. Buehler, J. Currey, P. Fratzl, H. S. Gupta, G. A. Holzapfel, D. J. S. Hulmes, R. F. Ker, M. Kjær, W. J. Landis, S. P. Magnusson, K. M. Meek, P. P. Purslow, E. A. Sander, F. H. Silver, T. J. Wess and P. Zaslansky, *Collagen: Structure and Mechanics*, Springer Science + Business Media, LLC 1 edition (May 30, 2008), New York, US, 2008.

32 P. Fagerholm, N. S. Lagali, K. Merrett, W. B. Jackson, R. Munger, Y. Liu, J. W. Polarek, M. Söderqvist and M. Griffith, *Sci. Transl. Med.*, 2010, **2**, 46ra61.

33 Y. Liu, L. Gan, D. J. Carlsson, P. Fagerholm, N. Lagali, M. A. Watsky, R. Munger, W. G. Hodge, D. Priest and M. Griffith, *Invest. Ophthalmol. Visual Sci.*, 2006, **47**, 1869–1875.

34 M. A. Wikler, *Performance standards for antimicrobial susceptibility testing: fifteenth informational supplement*, Clinical and Laboratory Standards Institute, Wayne, Pa. USA, 2005.

35 Lyophilization and aqueous reconstitution of collagen-stabilized AgNPs did not show any significant change in the position of the AgNP absorption band for AgNPs (Fig. S1†), indicating that neither particle size nor the protection conferred by the protein was modified by solvent evaporation (see Fig. 1A†). The SPB intensity (based on the area under the curve) decreased by less than 10%, indicating good material stability (Fig. S1†).

36 Calculations for the theoretical absorbance of the hydrogel containing 1.0 μM AgNPs, at 500 μm thickness, render a value of 1.7 that agrees with that measured for the prepared materials. Note that no color was observed after the injection of either $AgNO_3$ or HEBA (I-2959 photoproduct) at the same concentrations presented in the AgNP stock solution (data not shown).

37 A. B. G. Lansdown, *Adv. Pharmacol. Sci.*, 2010, **2010**, 16.

38 H. de Alwis Weerasekera, M. Griffith and E. I. Alarcon, in *Silver Nanoparticle Applications: In the Fabrication and Design of Medical and Biosensing Devices*, ed. E. I. Alarcon, K. Udekwu and M. Griffith, Springer International Publishing, UK, 2015, ch. 5, pp. 93–125, DOI: 10.1007/978-3-319-11262-6.

39 Q. L. Feng, J. Wu, G. Q. Chen, F. Z. Cui, T. N. Kim and J. O. Kim, *J. Biomed. Mater. Res.*, 2000, **52**, 662–668.

40 Total silver concentration for the silver nitrate impregnated material was ≈ 40 and 25 folds higher than that released from the 0.2 μM and 0.4 μM AgNP hydrogels; 339 (3.6 μM), 8.9 (0.08 μM) and 13 (0.12 μM) μg $L^{-1}$ for the impregnated, 0.2 μM and 0.4 μM AgNP hydrogels, respectively.

41 J. H. Merritt, D. E. Kadouri and G. A. O'Toole, *Current protocols in microbiology*, 2005, ch. 1, Unit 1B.1.

42 K. K. Comfort, L. K. Braydich-Stolle, E. I. Maurer and S. M. Hussain, *ACS Nano*, 2014, **8**, 3260–3271.

43 X. Liu, P. y. Lee, C. m. Ho, V. C. H. Lui, Y. Chen, C. m. Che, P. K. H. Tam and K. K. Y. Wong, *ChemMedChem*, 2010, **5**, 468–475.

44 S. Zhang, X. Liu, H. Wang, J. Peng and K. K. Y. Wong, *J. Pediatr. Surg.*, 2014, **49**, 606–613.

45 K. K. Y. Wong, S. O. F. Cheung, L. Huang, J. Niu, C. Tao, C. M. Ho, C. M. Che and P. K. H. Tam, *ChemMedChem*, 2009, **4**, 1129–1135.

46 G. Danscher and L. Locht, *Histochem. Cell Biol.*, 2010, **133**, 359–366.

47 J. Tang, L. Xiong, S. Wang, J. Wang, L. Liu, J. Li, F. Yuan and T. Xi, *J. Nanosci. Nanotechnol.*, 2009, **9**, 4924–4932.

48 M. Demoy, S. Gibaud, J. Andreux, C. Weingarten, B. Gouritin and P. Couvreur, *Pharm. Res.*, 1997, **14**, 463–468.

 